

## TETRAFIBRICIN, A NOVEL FIBRINOGEN RECEPTOR ANTAGONIST

## II. STRUCTURAL ELUCIDATION

TSUTOMU KAMIYAMA, YOSHIKO ITEZONO, TAKAYUKI UMINO, TOMOKO SATOH,  
NOBORU NAKAYAMA and KAZUTERU YOKOSE

Nippon Roche Research Center,  
200 Kajiwara, Kamakura, Kanagawa 247, Japan

(Received for publication January 25, 1993)

The structure of tetrafibricin, a novel and potent fibrinogen receptor antagonist isolated from the culture broth of *Streptomyces neyagawaensis* NR0577, was determined. Tetrafibricin has a unique structure containing primary amine, conjugated tetraenoic acid, and polyhydroxy functionalities that is biosynthetically related to the polyene macrolide antibiotics.

As described in the preceding paper, tetrafibricin was a new metabolite produced by *Streptomyces neyagawaensis* NR0577, which potently inhibited fibrinogen binding to its receptors. In this paper, we report on the structural elucidation of tetrafibricin.

## Results

## The Structure of Tetrafibricin

Tetrafibricin (**1**) was obtained as a pale yellow powder from the fermentation broth of the strain NR0577 by isolation procedures described in the preceding paper<sup>1</sup>. The molecular formula of **1** (Fig. 1) was determined to be  $C_{41}H_{67}NO_{13}$  from HRFAB-MS (Calcd: 782.4691, Found:  $m/z$  782.4676 ( $M+H$ )<sup>+</sup>) and <sup>13</sup>C NMR spectral data. Positive color reactions to ninhydrin and 2,4-dinitrophenylhydrazine suggested the presence of primary amino and carbonyl groups, respectively. The IR spectral data of **1** suggested the presence of carboxyl and/or carbonyl ( $3000\sim 2500$ ,  $1710\text{ cm}^{-1}$ ) and hydroxy and/or amino ( $3400$ ,  $1100\sim 1000\text{ cm}^{-1}$ ) functionalities. The UV spectral data [ $\lambda_{\text{max}}$  ( $H_2O$ ) 229 nm ( $\epsilon$  4,200), 323 nm ( $\epsilon$  48,400);  $\lambda_{\text{max}}$  (0.05 N HCl) 235 nm ( $\epsilon$  3,700), 339 nm ( $\epsilon$  43,500);  $\lambda_{\text{max}}$  (0.05 N NaOH) 229 nm ( $\epsilon$  4,100), 322 nm ( $\epsilon$  43,900)] indicated the presence of a conjugated tetraenoic acid chromophore<sup>2</sup>.

The structural elucidation of **1** was mainly carried out with various NMR experiments. Since **1** was

Fig. 1. The structure of tetrafibricin.

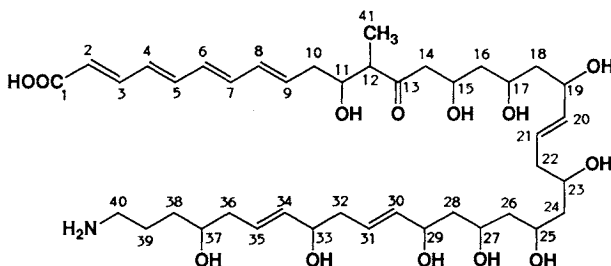
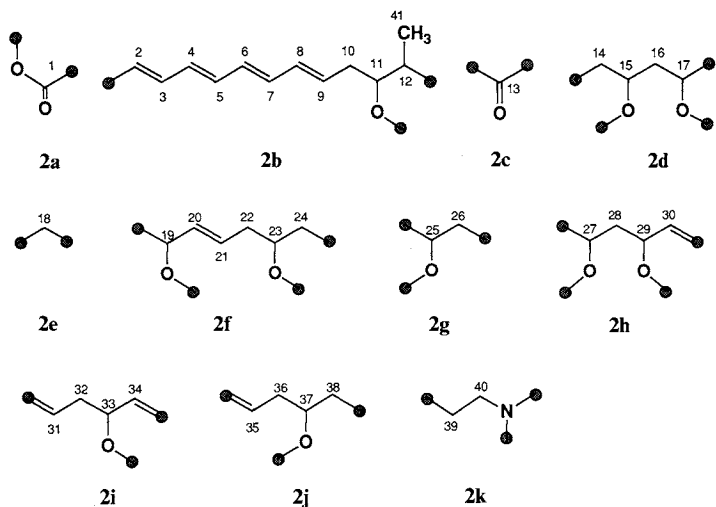


Table 1.  $^1\text{H}$  and  $^{13}\text{C}$  NMR data for **1** and **4**.

Position	<b>1</b> (in $\text{D}_2\text{O}$ )		<b>4</b> (in $\text{DMSO}-d_6$ )	
	$^{13}\text{C}^a$	$^1\text{H}^b$	$^{13}\text{C}$	$^1\text{H}$
1	178.6 s <sup>c</sup>		166.6 s <sup>c</sup>	
2	130.0 d	5.93 d (15.2)	119.3 d	5.95 d (15.2)
3	144.1 d	7.03 dd (15.2, 11.0)	144.8 d	7.29 dd (15.2, 11.6)
4	133.7 d	6.42 dd (15.2, 11.0)	129.1 d	6.43 dd (15.2, 11.6)
5	141.6 d	6.62 dd (15.2, 11.0)	141.5 d	6.77 dd (15.2, 11.2)
6	134.2 d	6.33 dd (15.2, 11.0)	129.8 d	6.29 dd (15.2, 11.2)
7	138.5 d	6.43 dd (15.2, 11.0)	137.8 d	6.47 dd (15.2, 11.2)
8	136.1 d	6.25 dd (15.2, 11.0)	131.5 d	6.20 dd (15.2, 11.2)
9	135.3 d	5.78 dt (15.2, 6.2)	136.1 d	5.90 quintet. (7.6)
10	41.3 t	2.36 m <sup>d</sup> , 2.32 m <sup>d</sup>	38.6 t	2.25 br t (6.8)
11	73.9 d	4.02 m <sup>d</sup>	72.3 d	3.60 m <sup>d</sup>
12	54.5 d	2.74 m <sup>d</sup>	41.8 t	1.34 m <sup>d</sup>
13	219.0 s		71.1 d	3.74 m <sup>d</sup>
14	51.6 t	2.82 dd (17.0, 8.8)	41.9 t	1.47 m <sup>d</sup>
		2.71 dd (17.0, 3.2)		
15	68.3 d	4.18 m <sup>d</sup>	67.8 d	3.74 m <sup>d</sup>
16	46.1 t	1.72 m <sup>d</sup>	44.6 t	1.36 m <sup>d</sup>
17	70.0 d	3.76 m <sup>d</sup>	67.2 d	3.72 m <sup>d</sup>
18	46.0 t	1.60 m <sup>d</sup>	45.0 t	1.47 m <sup>d</sup>
19	73.1 d	4.25 m <sup>d</sup>	69.4 d	4.06 m <sup>d</sup>
20	137.1 d	5.52 dd (15.5, 7.6)	135.6 d	5.40 dd (15.5, 6.8)
21	132.0 d	5.73 dt (15.5, 6.3)	126.3 d	5.58 dt (15.5, 7.0)
22	42.6 t	2.24 m <sup>d</sup>	40.9 t	2.06 m <sup>d</sup>
23	70.3 d	3.93 m <sup>d</sup>	66.8 d	3.68 m <sup>d</sup>
24	46.3 t	1.52 m <sup>d</sup>	44.8 t	1.27 m <sup>d</sup>
25	67.6 d	3.97 m <sup>d</sup>	63.9 d	3.89 m <sup>d</sup>
26	47.4 t	1.66 m <sup>d</sup>	45.9 t	1.32 m <sup>d</sup>
27	67.6 d	3.97 m <sup>d</sup>	63.8 d	3.89 m <sup>d</sup>
28	46.9 t	1.60 m <sup>d</sup>	45.7 t	1.37 m <sup>d</sup>
29	71.9 d	4.26 m <sup>d</sup>	67.7 d	4.09 m <sup>d</sup>
30	138.0 d	5.58 dd (15.5, 5.2)	136.6 d	5.44 dd (15.5, 6.8)
31	130.2 d	5.66 dt (15.5, 6.6)	125.0 d	5.51 dd (15.5, 6.0)
32	42.1 t	2.30 t (6.6)	40.5 t	2.10 m <sup>d</sup>
33	74.6 d	4.15 br t (6.0)	70.9 d	3.89 m <sup>d</sup>
34	137.2 d	5.55 dd (15.5, 6.8)	135.4 d	5.42 dd (15.5, 6.8)
35	131.0 d	5.67 dt (15.5, 6.8)	126.3 d	5.56 dt (15.5, 7.0)
36	41.9 t	2.22 m <sup>d</sup>	40.2 t	2.06 m <sup>d</sup>
37	73.1 d	3.70 m <sup>d</sup>	69.5 d	3.41 m <sup>d</sup>
38	35.2 t	1.60 m <sup>d</sup> , 1.50 m <sup>d</sup>	33.7 t	1.23 m <sup>d</sup> , 1.36 m <sup>d</sup>
39	26.1 t	1.75 m <sup>d</sup>	25.5 t	1.37 m <sup>d</sup> , 1.48 m <sup>d</sup>
40	42.4 t	2.98 ddd (7.6, 7.1, 2.2)	38.9 t	3.00 dt (6.0, 6.8)
41	13.4 q	1.08 d (7.1)	7.5 q	0.82 d (6.8)
1-OCH <sub>3</sub>			51.2 q	3.66 s
41-NAc			168.8 s	
			22.6 q	1.78 s
11-OH				4.47 d (4.4)
13-OH				4.47 d (3.0)
15-OH				4.67 d (4.4)
17-OH				4.60 d (4.4)
19-OH				4.68 d (4.4)
23-OH				4.30 d (5.2)
25-OH				4.22 d (5.2)
27-OH				4.26 d (5.6)
29-OH				4.51 d (5.2)
33-OH				4.59 d (4.4)
37-OH				4.38 d (5.2)
30-NH				7.76 br t (6.0)

<sup>a</sup> 100 MHz;  $\delta$  in ppm.<sup>b</sup> 400 MHz;  $\delta$  in ppm,  $J$  in Hz.<sup>c</sup> Assigned by DEPT experiments.<sup>d</sup> Overlapping signals.

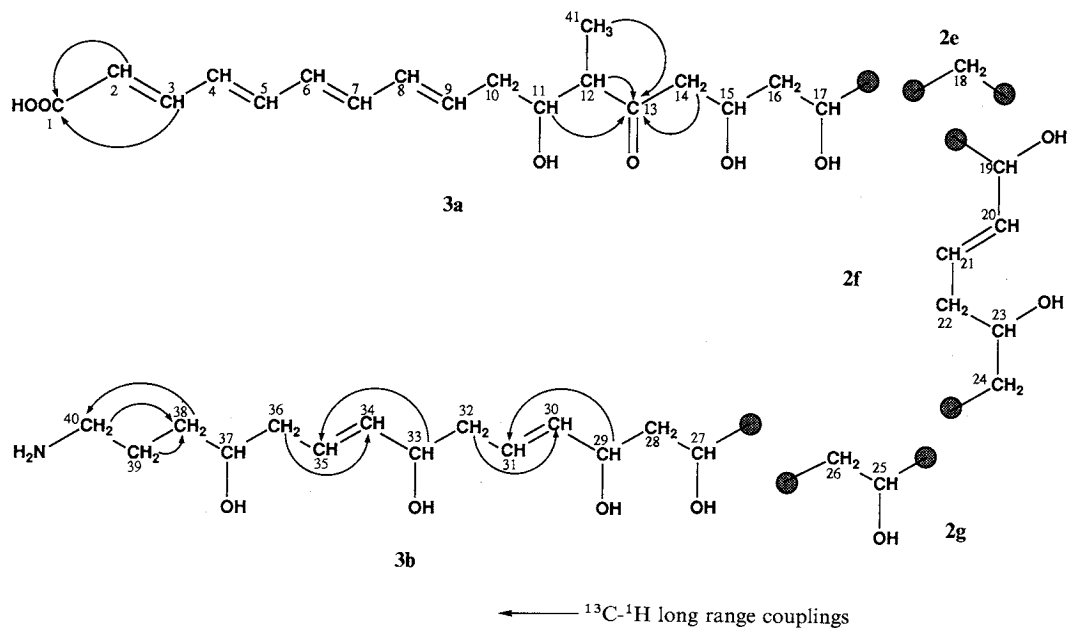
Fig. 2. Partial structures elucidated from  $^1\text{H}$  and  $^{13}\text{C}$  NMR,  $^1\text{H}$ - $^1\text{H}$  COSY and HSQC experiments.

unstable in  $\text{DMSO}-d_6$ , a  $\text{D}_2\text{O}$  solution of **1** purged with argon was used for the NMR experiments. The  $^1\text{H}$  and  $^{13}\text{C}$  NMR spectral data in  $\text{D}_2\text{O}$  are shown in Table 1. Partial structures **2a**~**2k** (Fig. 2) were elucidated from the analyses of the  $^1\text{H}$  NMR,  $^{13}\text{C}$  NMR,  $^1\text{H}$ - $^1\text{H}$  COSY and HSQC<sup>3)</sup> experiments on **1**. These fragments were connected by  $^{13}\text{C}$ - $^1\text{H}$  long range couplings, obtained by the HMBC experiment. The  $^{13}\text{C}$ - $^1\text{H}$  long range couplings between C-1 (**2a** in Fig. 2) and 2-H and 3-H (**2b** in Fig. 2) indicated the linkage of C-1 and C-2 to form a tetraenoic acid chromophore. This functionality was corroborated by the characteristic UV absorption maxima at 229 nm ( $\epsilon$  4,200) and 323 nm ( $\epsilon$  48,300). The  $^{13}\text{C}$ - $^1\text{H}$  long range couplings between C-13 (**2c** in Fig. 2) and 11-H, 12-H, 41-H (**2b** in Fig. 2) and 14-H (**2d** in Fig. 2) indicated the linkage from C-12 to C-14. Thus, the partial structure **3a** was established, as shown in Fig. 3. The geometries of the four disubstituted double bonds in the partial structure **3a** were determined to be *2E*, *4E*, *6E* and *8E* on the basis of the coupling constants ( $J_{2,3}$ ,  $J_{4,5}$ ,  $J_{6,7}$  and  $J_{8,9} = 15.2$  Hz) observed among the olefinic protons.

The connectivities between C-30 (**2h** in Fig. 2) and C-31 (**2i** in Fig. 2) and between C-34 (**2i** in Fig. 2) and C-35 (**2j** in Fig. 2) positions were clarified by the analyses of selective coherence transfer experiments<sup>4,5)</sup>, because the olefinic proton signals of 30-H, 31-H, 34-H and 35-H contained in partial structures **2h**, **2i** and **2j** were not well interpreted by the  $^1\text{H}$ - $^1\text{H}$  COSY experiments. The linkages of C-30 and C-31, and of C-34 and C-35 were supported by the  $^{13}\text{C}$ - $^1\text{H}$  long range couplings between C-31 and 29-H, between C-30 and 32-H, between C-34 and 36-H, and between C-35 and 33-H in the HMBC experiments. The geometries of the two disubstituted double bonds in partial structure **3b** were determined to be *30E* and *34E* on the basis of the observed coupling constants ( $J_{30,31} = 15.5$  Hz and  $J_{34,35} = 15.5$  Hz). The  $^{13}\text{C}$ - $^1\text{H}$  long range couplings between C-38 (**2j** in Fig. 2) and 39-H and 40-H (**2k** in Fig. 2) and between C-40 (**2k** in Fig. 2) and 38-H (**2j** in Fig. 2) also indicated the linkage of C-38 and C-39. Thus, the partial structure **3b** containing partial structures **2h**, **2i**, **2j**, and **2k** was established as shown in Fig. 3.

With respect to the remaining partial structures **2e**, **2f** and **2g**, we could not connect each unit, or each unit with partial structures **3a** and **3b**, for the following reasons. 1) Since the cross peaks were severely overlapped at the aliphatic region in the  $^1\text{H}$ - $^1\text{H}$  COSY, HMBC, HOHAHA experiments, we could not

Fig. 3. Partial structures elucidated from the HMBC experiments.

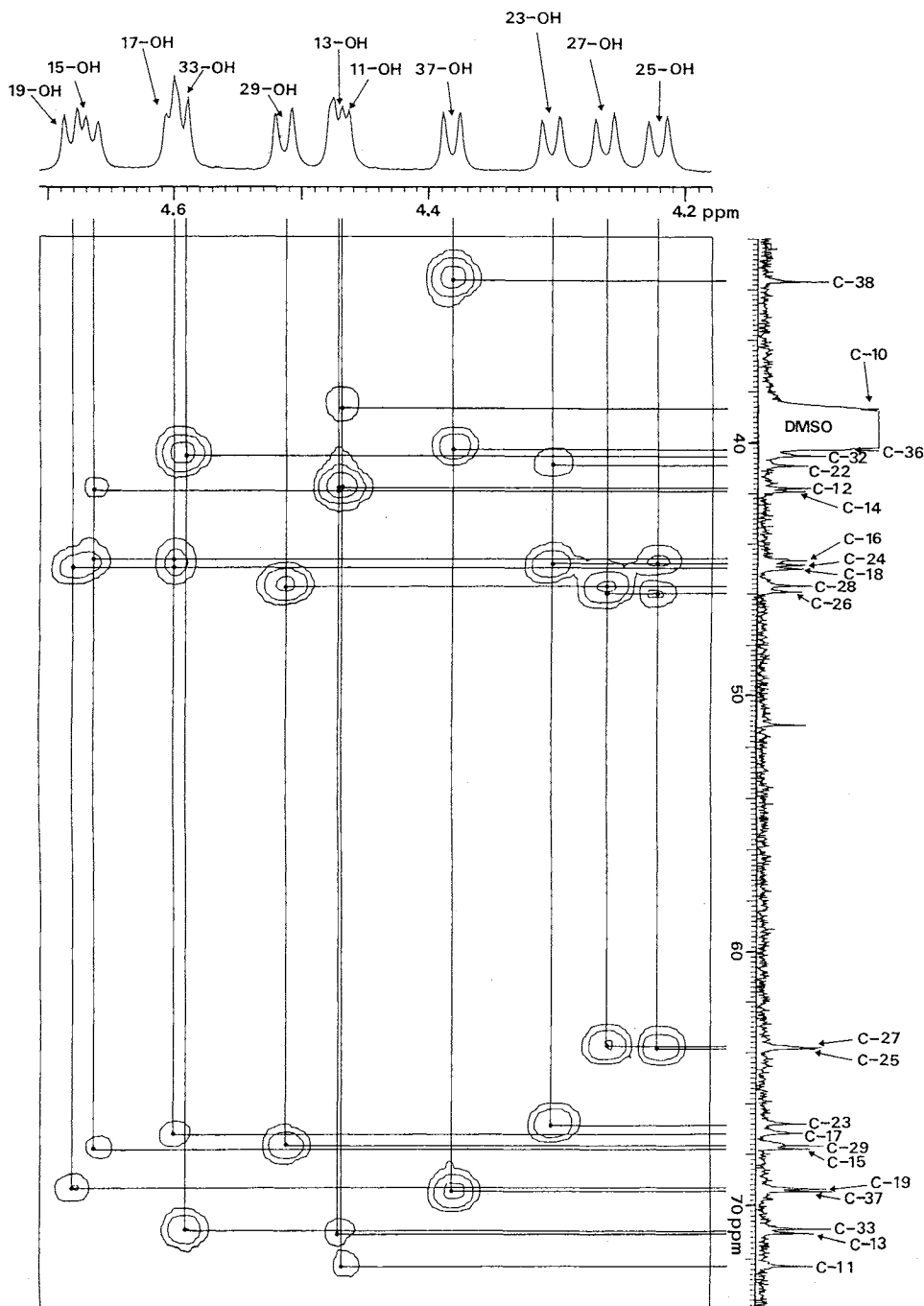


clearly distinguish the peaks of 18-H and 16-H. 2) Since the  $^1\text{H}$  and  $^{13}\text{C}$  chemical shifts at C-25 and C-27 positions were completely overlapped ( $\delta_{\text{H}}$  3.97,  $\delta_{\text{C}}$  67.6), the two alternative carbon sequences (C-24–C-25–C-26–C-27) and (C-24–C-26–C-25–C-27) were possible. The geometry of the double bond (C-20 and C-21) in **2f** was determined to be *E* based on the vicinal coupling constant ( $J_{20,21} = 15.5$  Hz).

To determine the connectivities of the remaining unsolved parts, we prepared *N*-acetyldihydro-tetrafabricin methyl ester, which was more stable than **1**, so that we could carry out the NMR experiments in  $\text{DMSO}-d_6$  solution and observed the  $^{13}\text{C}-^1\text{H}$  long range couplings between the hydroxy protons and carbons.

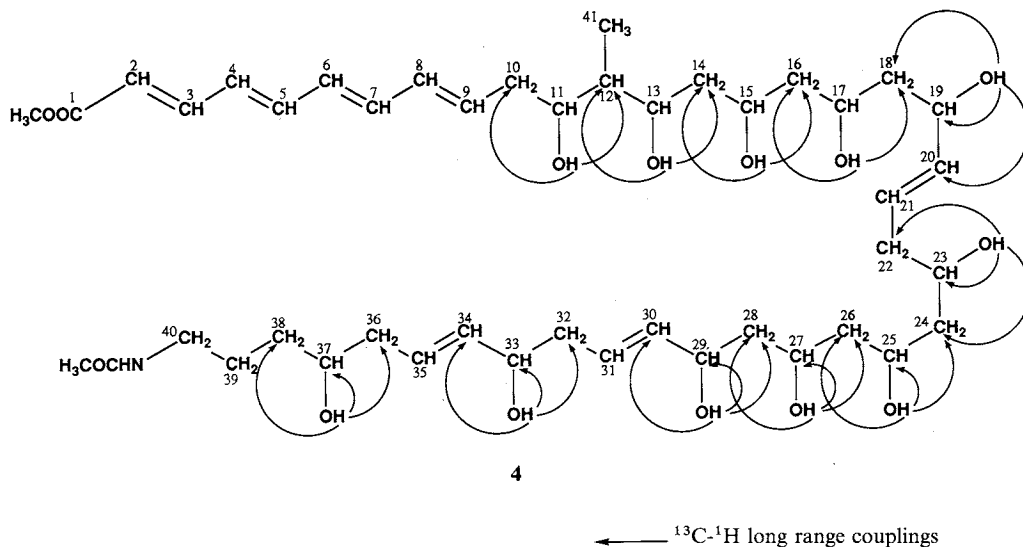
#### The Structure of *N*-Acetyldihydro-tetrafabricin Methyl Ester

*N*-Acetyldihydro-tetrafabricin methyl ester (**4**) was obtained from **1** by the following procedures: 1) Reduction by  $\text{NaBH}_4$  in  $\text{H}_2\text{O}$ ; 2) trimethylsilyldiazomethane treatment in  $\text{MeOH}$ ; and 3) acetylation with  $\text{Ac}_2\text{O}$  in  $\text{THF}-\text{H}_2\text{O}$ . Since two epimers, **4** and **5**, were obtained by the above derivatizations, each epimer was isolated by preparative HPLC (ODS). The molecular formula ( $\text{C}_{44}\text{H}_{73}\text{NO}_{14}$ ) of the major product, **4**, was determined from the analyses of the positive ion HRFAB-MS (Found:  $(\text{M} + \text{Na})^+$   $m/z$  862.4912; calcd for  $(\text{C}_{44}\text{H}_{73}\text{NO}_{14}\text{Na})$ : 862.4929) and the  $^1\text{H}$  and  $^{13}\text{C}$  NMR spectral data. In the  $^1\text{H}$  and  $^{13}\text{C}$  NMR spectra of **4** in  $\text{DMSO}-d_6$ , one *N*-acetyl signal ( $\delta_{\text{C}}$  168.8, 22.6 and  $\delta_{\text{H}}$  1.78 (3H), 7.76 (NH)), one ester methyl signal ( $\delta_{\text{C}}$  51.2 and  $\delta_{\text{H}}$  3.66 (3H)) and one methine signal ( $\delta_{\text{C}}$  71.1 and  $\delta_{\text{H}}$  3.74) instead of the carbonyl carbon signal of **1** ( $\delta_{\text{C}}$  219.0 in **1**) were observed indicating that **4** was an *N*-acetyl and methyl ester derivative of dihydro-tetrafabricin. The  $^1\text{H}$  and  $^{13}\text{C}$  NMR spectral data of **4** are shown in Table 1. The analyses of  $^1\text{H}$  and  $^{13}\text{C}$  NMR, DEPT,  $^1\text{H}-^1\text{H}$  COSY, HSQC, and HMBC experiments on **4** in  $\text{DMSO}-d_6$  led to the determination of the remaining connectivities. The carbon sequences from C-17 to C-19, and from C-24 to C-27 were determined by the analysis of the  $^{13}\text{C}-^1\text{H}$  long range couplings between hydrogen atoms of the hydroxy groups and their  $\alpha$ - and  $\beta$ -carbons observed in the HMBC experiments (Figs. 4 and 5). The

Fig. 4. HMBC spectrum of 4 (partial, in DMSO- $d_6$ ).

$^{13}\text{C}$ - $^1\text{H}$  long range couplings between 25-OH ( $\delta_{\text{H}}$  4.22) and C-24 ( $\delta_{\text{C}}$  44.8), C-25 ( $\delta_{\text{C}}$  63.9) and C-26 ( $\delta_{\text{C}}$  45.9), and also between 27-OH ( $\delta_{\text{H}}$  4.26) and C-26 ( $\delta_{\text{C}}$  45.9), C-27 ( $\delta_{\text{C}}$  63.8) and C-28 ( $\delta_{\text{C}}$  45.7) indicated the linkage from C-24 to C-27. By repeating the same procedure, the  $^{13}\text{C}$ - $^1\text{H}$  long range couplings between 17-OH ( $\delta_{\text{H}}$  4.60) and C-16 ( $\delta_{\text{C}}$  44.6), C-17 ( $\delta_{\text{C}}$  67.2) and C-18 ( $\delta_{\text{C}}$  45.0), as well as between 19-OH ( $\delta_{\text{H}}$  4.68)

Fig. 5. The structure of **4** and the  $^{13}\text{C}$ - $^1\text{H}$  long range couplings observed in the HMBC experiments.



and C-18 ( $\delta_{\text{C}}$  45.0), C-19 ( $\delta_{\text{C}}$  69.4) and C-20 ( $\delta_{\text{C}}$  135.6) also indicated the linkage from C-17 to C-19. Thus, the structure of **4** was established as shown in Fig. 5.

The structure of tetrafibricin was deduced from the derivative **4** and determined to be **1**, as shown in Fig. 1. The stereochemical studies will be completed in due course.

### Discussion

Several fibrinogen receptor antagonists of natural origin have been reported. Decorsin<sup>6</sup>) isolated from the North American leech, *Macrobdella decora*, and disintegrins such as echistatin<sup>7</sup>), kistrin<sup>8</sup>), trigramin<sup>8</sup>) and bitan<sup>8</sup>) isolated from the venom of various snakes are peptide molecules containing the RGD (Arg-Gly-Asp) sequence.

Tetrafibricin is completely different from other known fibrinogen receptor antagonists derived from natural products and has a unique structure containing primary amine, conjugated tetraenoic acid, and polyhydroxy functionalities that is found to be closely related to the polyene macrolide antibiotic, lienomycin<sup>9</sup>). However, tetrafibricin does not have a macrocyclic lactone structure and is inactive against *Bacillus subtilis* and *Escherichia coli*. Since tetrafibricin is a non-peptidic antagonist of fibrinogen receptors, it will be a good tool to study fibrinogen-binding and platelet aggregation.

### Experimental

$^1\text{H}$  and  $^{13}\text{C}$  NMR spectra were recorded on a JEOL JNM-GSX-400 NMR spectrometer at 400 and 100 MHz, respectively, using TMS or sodium 3-(trimethylsilyl)-propionate- $d_4$  (in  $\text{D}_2\text{O}$ ) as an internal standard. UV spectra were recorded on a Kontron Uvikon 860 UV spectrometer. FAB-MS were measured on a JEOL JMS-DX-303/system 5000 mass spectrometer. Optical rotation was measured on a JASCO FIP-140 digital polarimeter. TLC was performed on HPTLC plate RP-18 (E. Merck, Art. No. 13124), and spots were visualized with UV light or ninhydrin spray. The solvent used for TLC was a mixture of MeOH and 50 mM aqueous  $\text{Na}_2\text{HPO}_4$  (2:1).

#### Synthesis of *N*-Acetyldihydrotetrafibricin Methyl Ester **4** and Its Epimer **5**

Since dihydrotetrafibricin and dihydrotetrafibricin methyl ester were very unstable in air and light,

we carried out the following reactions without isolation. The reactions were monitored by FAB-MS, TLC analyses, and color reactions. All the reactions proceeded under argon atmosphere using amber glassware.

To a solution of **1** (47 mg) in water (3 ml) was added NaBH<sub>4</sub> (20 mg), and the mixture was stirred for 1 hour at 0°C. The reaction mixture was neutralized with 0.1 N HCl and applied onto a column (1.5 ml) of MCI GEL CHP-20P. The column was washed with water and then eluted with 50% aqueous acetone. The eluate was concentrated under reduced pressure to give dihydrotetrafabricin (31.7 mg) (TLC: Rf 0.58; FAB-MS: *m/z* 784 (M+H)<sup>+</sup>, 805 (M+Na)<sup>+</sup>).

To a solution of dihydrotetrafabricin in MeOH (20 ml) was added 1.5 ml of trimethylsilyldiazomethane (10% in hexane) (Tokyo Kasei Kogyo Co., Ltd.), the mixture was stirred for 1 hour at 0°C. The reaction mixture was concentrated under reduced pressure to give dihydrotetrafabricin methyl ester (32 mg) (TLC: Rf 0.40; FAB-MS: *m/z* 798 (M+H)<sup>+</sup>).

To a solution of dihydrotetrafabricin methyl ester in H<sub>2</sub>O (1 ml) and THF (5 ml) was added acetic anhydride (10 μl), and the mixture was stirred for 30 minutes at room temperature. The reaction mixture was purified by HPLC with YMC pack D-ODS-10 (2.4 cm i.d. × 25 cm) and eluted with 55% aqueous MeOH at a flow rate of 25 ml/minute. *N*-Acetyldihydrotetrafabricin methyl ester **4** and its epimer **5** detected by UV absorption at 340 nm produced peaks at 15 and 19 minutes, respectively. Each eluate containing **4** or **5** was concentrated under reduced pressure to give 7.0 and 2.3 mg, respectively, as a colorless powder.

**4**: HRFAB-MS: *m/z* 862.4912 (M+Na)<sup>+</sup>, (−1.7 mmu error); UV λ<sub>max</sub><sup>MeOH</sup> nm (ε): 229 (4,400), 333 (52,200); [α]<sub>D</sub><sup>24</sup>: −13.9° (c 0.35, MeOH); <sup>1</sup>H and <sup>13</sup>C NMR data for **4** are shown in Table 1.

**5**: FAB-MS: *m/z* 862 (M+Na)<sup>+</sup>, UV λ<sub>max</sub><sup>MeOH</sup> nm (ε): 229 (4,200), 333 (51,100); [α]<sub>D</sub><sup>24</sup>: −31.4° (c 0.21, MeOH); <sup>1</sup>H NMR (400 MHz, DMSO-*d*<sub>6</sub>): δ<sub>H</sub> 0.77 (3H, d, *J*=6.8 Hz), 1.23~1.49 (17H), 1.78 (3H, s), 2.03~2.12 (6H), 2.24 (2H, quintet, *J*=6.8 Hz), 2.99 (2H, br q, *J*=6.0 Hz), 3.42 (1H, m), 3.66 (3H, s), 3.72 (3H), 3.88 (5H), 4.09 (2H), 4.22 (1H, d, *J*=4.8 Hz), 4.26 (1H, d, *J*=5.2 Hz), 4.30 (1H, d, *J*=5.2 Hz), 4.33 (1H, d, *J*=5.2 Hz), 4.37 (1H, d, *J*=4.8 Hz), 4.40 (1H, d, *J*=4.5 Hz), 4.46 (1H, d, *J*=4.0 Hz), 4.50 (1H, d, *J*=4.0 Hz), 4.59 (2H, d, *J*=2.8 Hz), 4.67 (1H, br s), 5.40 (1H, dd, *J*=15.5, 6.8 Hz), 5.42 (1H, dd, *J*=15.5, 6.8 Hz), 5.44 (1H, dd, *J*=15.5, 6.8 Hz), 5.51 (1H, dt, *J*=15.5, 6.0 Hz), 5.56 (1H, dt, *J*=15.5, 7.0 Hz), 5.58 (1H, dt, *J*=15.5, 7.0 Hz), 5.91 (1H, quintet, *J*=7.6 Hz), 5.95 (1H, d, *J*=15.2 Hz), 6.20 (1H, dd, *J*=15.2, 11.2 Hz), 6.29 (1H, d, *J*=15.2, 11.2 Hz), 6.44 (1H, dd, *J*=15.2, 11.2 Hz), 6.48 (1H, dd, *J*=15.2, 11.2 Hz), 6.77 (1H, dd, *J*=15.2, 11.2 Hz), 7.29 (1H, dd, *J*=15.2, 11.2 Hz), 7.76 (1H, br t, *J*=6 Hz); <sup>13</sup>C NMR (100 MHz, DMSO-*d*<sub>6</sub>): δ<sub>C</sub> s: 168.8, 166.6, d: 144.7, 141.5, 137.8, 136.6, 136.2, 135.6, 135.4, 131.4, 129.7, 129.1, 126.3 × 2, 125.0, 119.3, 70.8, 69.7, 69.4 × 2, 68.8, 67.6, 67.3, 66.8, 65.9, 63.9, 63.8, 42.8, t: 45.9, 45.7, 45.3, 45.0, 44.8, 41.9, 40.8, 40.5, 40.1, 38.6, 38.5, 33.7, 25.4, q: 51.1, 22.5, 9.8.

#### References

- 1) KAMIYAMA, T.; T. UMINO, N. FUJISAKI, K. FUJIMORI, T. SATOH, Y. YAMASHITA, S. OHSHIMA, J. WATANABE & K. YOKOSE: Tetrafabricin, a novel fibrinogen receptor antagonist. I. Taxonomy, fermentation, isolation, characterization and biological activities. *J. Antibiotics* 46: 1039~1046, 1993
- 2) HAUSSER, K. W.; R. KUHN, A. SMAKULA & M. HOFFER: Lichtabsorption und doppelbindung. II. Polyenaldehyde und polyenecarbonsäuren. *Z. Physik. Chem.* B29: 371~377, 1935
- 3) NORWOOD, T. J.; J. BOYD, J. E. HERITAGE, N. SOFFE & I. D. CAMPBELL: Comparison of techniques for <sup>1</sup>H-detected heteronuclear <sup>1</sup>H-<sup>15</sup>N spectroscopy. *J. Magn. Reson.* 87: 488~501, 1990
- 4) MILLOT, C.; J. BRONDEAU & D. CANET: Determination of mutual coupling in <sup>1</sup>H NMR spectra by semiselective excitation. *J. Magn. Reson.* 58: 143~148, 1984
- 5) BAUER, C.; R. FREEMAN, T. FRENKIEL, J. KEELER & A. J. SHAKA: Gaussian pulses. *J. Magn. Reson.* 58: 442~457, 1984
- 6) SEYMOUR, J. L.; W. J. HENZEL, B. NEVINS, J. T. STULTS & R. A. LAZARUS: Decorsin, a potent glycoprotein IIb-IIIa antagonist and platelet aggregation inhibitor from the Leech *Macrobdella decora*. *J. Biol. Chem.* 265: 10143~10147, 1990
- 7) GAN, Z. R.; R. J. GOULD, J. W. JACOBS, P. A. FRIEDMAN & M. A. POLOKOFF: Echistatin, a potent platelet aggregation inhibitor from the venom of the viper, *Echis carinatus*. *J. Biol. Chem.* 263: 19827~19832, 1988
- 8) DENNIS, M. S.; W. J. HENZEL, R. M. PITTI, M. T. LIPARI, M. A. NAPIER, T. A. DEISHER, S. BUNTING & R. A.

- LAZARUS: Platelet glycoprotein IIb-IIIa protein antagonists from snake venoms: Evidence for a family of platelet-aggregation inhibitors. *Proc. Natl. Acad. Sci. U.S.A.* 87: 2471~2475, 1989
- 9) PAWLAK, J.; K. NAKANISHI, T. IWASHITA & E. BOROWSKI: Stereochemical studies of polyols from the polyene macrolide lienomycin. *J. Org. Chem.* 52: 2896~2901, 1987